

Echo-enabled harmonic generation for seeded FELs

G. Stupakov

SLAC National Accelerator Laboratory, Menlo Park, CA, USA

ABSTRACT

In the x-ray wavelengths, the two leading FEL concepts are the self-amplified spontaneous emission (SASE) configuration and the high-gain harmonic generation (HGHG) scheme. While the radiation from a SASE FEL is coherent transversely, it typically has rather limited temporal coherence. Alternatively, the HGHG scheme allows generation of fully coherent radiation by up-converting the frequency of a high-power seed laser. However, due to the relatively low up-frequency conversion efficiency, multiple stages of HGHG FEL are needed in order to generate x-rays from a UV laser. The up-frequency conversion efficiency can be greatly improved with the recently proposed echo-enabled harmonic generation (EEHG) technique. In this work we will present the concept of EEHG, and address some practically important issues that affect the performance of the seeding. We show how the EEHG can be incorporated in the FEL scheme and what is the expected performance of the EEHG seeded FEL. We will then briefly describe the first proof-of-principle EEHG experiment carried out at the Next Linear Collider Test Accelerator (NLCTA) at SLAC. We will also discuss latest advances in the echo-scheme approach, and refer to subsequent modifications of the original concept.

Keywords: Free electron laser, seeding, EEHG, x-ray

1. INTRODUCTION

There has been continually growing interests in generating coherent and powerful short wavelength radiation using the free electron laser (FEL) scheme, as reflected by the many proposals and funded projects worldwide.¹ In the nanometer and sub-nanometer wavelengths, the two leading candidates are self-amplified spontaneous emission (SASE) configuration^{2,3} and the high gain harmonic generation (HGHG) scheme.^{4,5} Since the SASE FEL starts from electron beam shot noise, its output typically has limited temporal coherence and relatively large shot-to-shot fluctuations in both the power and the spectrum. An alternative to SASE configuration is the HGHG scheme that allows generation of temporally coherent radiation by using up-frequency conversion of a high-power seeding signal.

In the classic HGHG scheme,⁵ the electron beam is first energy modulated with a seed laser in the undulator (modulator) and then sent through a dispersion region which converts the energy modulation into a density modulation. The density modulated beam is then sent through the second undulator (radiator) tuned at some harmonic of the seed laser. The up-frequency conversion efficiency for this classic HGHG scheme is relatively low: generation of n th harmonic of the seed laser requires the energy modulation amplitude approximately equal to n times the slice energy spread of the beam. Because a considerable increase of the slice energy spread would degrade the lasing process in the radiator, the harmonic numbers n used in the classic HGHG scheme are typically no larger than 6. In order to generate coherent soft x-rays with a wavelength in the range of few nanometers using an ultra-violet (UV) seeding laser with the wavelength ~ 200 nm, multiple stages of the classic HGHG FEL are to be used.⁶

Recently a new method for generation of high harmonics using the beam echo effect was proposed.⁷ The echo scheme has a remarkable up-frequency conversion efficiency and allows for generation of high harmonics with a relatively small energy modulation. The echo scheme uses two modulators and two dispersion sections. In general, the frequencies of the first, ω_1 , and the second, ω_2 , modulators can be different. The beam modulation is observed at the wavelength $2\pi/k_{\text{echo}}$, where $ck_{\text{echo}} = n\omega_1 + m\omega_2$, with n and m integer numbers. The first dispersion section is chosen to be strong enough, so that the energy and the density modulations induced in the first modulator are macroscopically smeared due to the slippage effect. At the same time, this smearing introduces a complicated fine structure into the phase space of the beam. The echo then occurs as a recoherence effect caused by the mixing of the correlations between the modulation in the second modulator and the structures

imprinted onto the phase space by the combined effect of the first modulator and the first dispersion section. The key advantage of the echo scheme is that the amplitude of high harmonics of the echo is a slow decaying function of the harmonic number.

2. PRINCIPLES OF EEHG FEL

The schematic of the EEHG is shown in Fig. 1. The EEHG consists of two modulators and two dispersion sections. The system is followed by a radiator undulator (not shown in Fig. 1). Similar to the classic HGHG scheme, a laser pulse is used to modulate the beam energy in the first undulator, and then the beam passes through the first chicane. Subsequently a second laser pulse modulates the beam energy in the second undulator

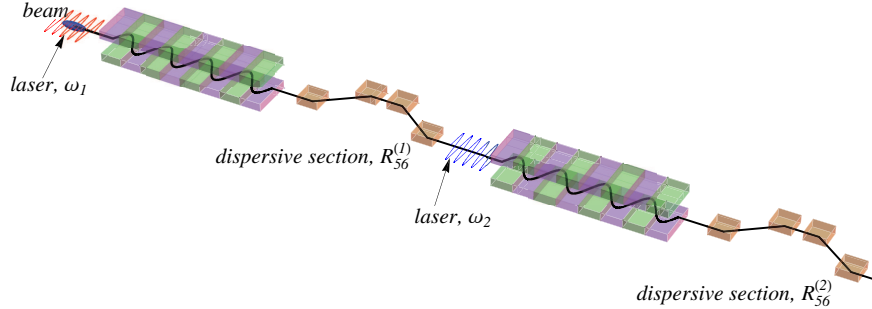


Figure 1. Schematic of the EEHG. The beam energy is modulated in the first undulator (modulator 1), tuned at frequency ω_1 , due to the interaction with the first laser beam. After passing through the first dispersion section with $R_{56}^{(1)}$, the beam energy is then modulated in the second undulator (modulator 2), tuned at frequency, ω_2 due to the interaction with the second laser beam. The beam then passes through the second dispersion section $R_{56}^{(2)}$.

and the beam passes through the second chicane. The laser frequencies for the first and the second modulators, ω_1 and ω_2 , in general case are different, but they can also be equal.

Calculations show⁷ that at the exit from the second chicane the beam is modulated in the longitudinal direction with the combination of frequencies ω_1 and ω_2 . More precisely, the modulations have wavenumbers $k_{n,m}$,

$$ck_{n,m} = n\omega_1 + m\omega_2, \quad (1)$$

where n and m are integer numbers. Numbers n and m can be either positive or negative, with a negative $k_{n,m}$ meaning a modulation with wavelength $2\pi/|k_{n,m}|$. Using the notation $b_{n,m}$ for the corresponding bunching factor, one finds⁸

$$b_{n,m} = |e^{-\frac{1}{2}(nB_1+(Km+n)B_2)^2} J_m(-(Km+n)A_2B_2) J_n(-A_1(nB_1+(Km+n)B_2))|, \quad (2)$$

where $A_1 = \Delta E_1/\sigma_E$, $B_1 = R_{56}^{(1)} k_1 \sigma_E/E_0$, $A_2 = \Delta E_2/\sigma_E$, $B_2 = R_{56}^{(2)} k_1 \sigma_E/E_0$, ΔE_1 and ΔE_2 are the amplitudes of the energy modulation in the first and second modulators, respectively, $R_{56}^{(1)}$ and $R_{56}^{(2)}$ are the R_{56} parameters for the first and second chicanes, $k_1 = \omega_1/c$, $K = \omega_2/\omega_1$, and J_n is the Bessel function of order n . In (2) we assumed a Gaussian energy distribution of the beam with the rms energy spread σ_E .

Having four dimensionless parameters A_1 , A_2 , B_1 , and B_2 in the problem allows one a much better optimization of the absolute value of the bunching factor $b_{n,m}$ for given n , m , and the ratio K of the frequencies. Analysis shows that the bunching factor attains its maximum when $n = \pm 1$ and decreases as the absolute value of n increases. In order for B_1 and B_2 to have the same sign, (which means that one can use either two chicanes

or two doglegs as dispersion elements), n and m need to have opposite signs. Limiting consideration to the case $n = -1$ and $m > 0$ only, one can try to choose the dispersion strengths B_1 and B_2 in such a way that they maximize the value of $b_{-1,m}$ for given amplitudes A_1 and A_2 and the number m . Such maximization was carried out in Ref.⁸ For $m > 4$, the optimal value of B_2 is given by $B_2 = (m + 0.81m^{1/3})/((Km - 1)A_2)$. After B_2 is found, the optimal value of B_1 is computed from $B_1 = (Km - 1)B_2 + \xi(A_1)$, where the function $\xi(A_1)$ should be determined from the equation $A_1 [J_0(A_1\xi) - J_2(A_1\xi)] = 2\xi J_1(A_1\xi)$. It turns out that the optimized bunching factor does not depend on A_2 and depends only on A_1 . This dependence is given by the following equation

$$b_{-1,m} \approx \frac{F(A_1)}{m^{1/3}}, \quad (3)$$

where the function $F(A_1)$ is shown in Fig. 2a. From Fig. 2a one sees that the maximal value of this function

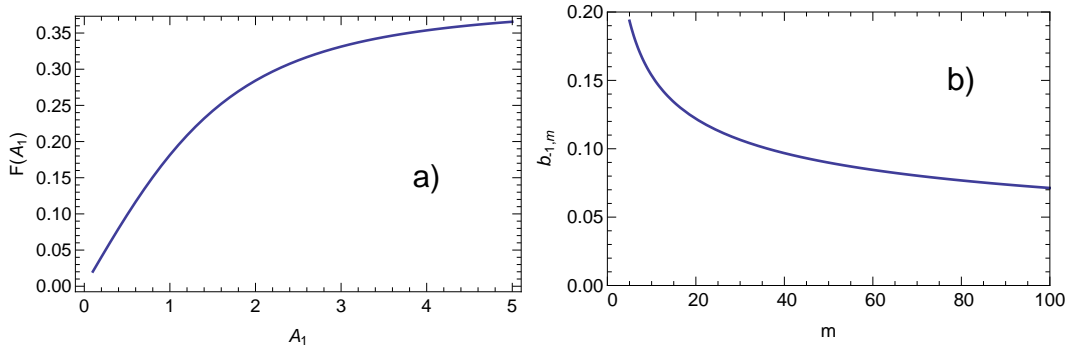


Figure 2. The dependence F from Eq. (3) versus A_1 (left panel) and the bunching factor $b_{-1,m}$ versus the harmonic number for $A_1 = 3$ (right panel).

increases linearly with A_1 when A_1 is smaller than 2. When A_1 becomes larger than 3, the growth of F slows down, and when A_1 tends to infinity, F approaches 0.39. In this limit the maximal bunching factor becomes (assuming $m > 4$)

$$b_{-1,m} \approx \frac{0.39}{m^{1/3}}. \quad (4)$$

Fig. 2b shows the optimized bunching factor as a function of the harmonic number for $A_1 = 3$: one can see that even at 100th harmonic the bunching factor is close to 7%.

3. ECHO PHASE SPACE

It is easy to show from the equations of the previous section that in the limit of large values of m , and assuming $A_1, A_2 \sim 1$,

$$B_2 \approx \frac{1}{KA_2}, \quad B_1 \approx \frac{m}{A_2}, \quad (5)$$

which means that the strength of the first chicane is much larger than the second one. The large value of $R_{56}^{(1)}$ results in dramatic changes of the longitudinal phase space of the beam. The phase space after the first and the second chicanes for $A_1 = 1$, $A_2 = 1$, $B_1 = 12.1$ and $B_2 = 1.3$ are shown in Fig. 3. The complicated structure of the phase space results from the fact that due to large slippage of particles with different energies, they end up at the same position z starting many wavelengths away from that position. Correspondingly, the energy distribution function becomes highly modulated in energy. The bands generated in the beam phase space after the first chicane are rotated by ninety degrees in their middle parts in such a way that their projections onto the z axis generate modulation of the beam density and current. The current modulation corresponding to Fig. 3 has the bunching factor $b_{10} \approx 0.08$ at the 10th harmonic of the laser frequency.

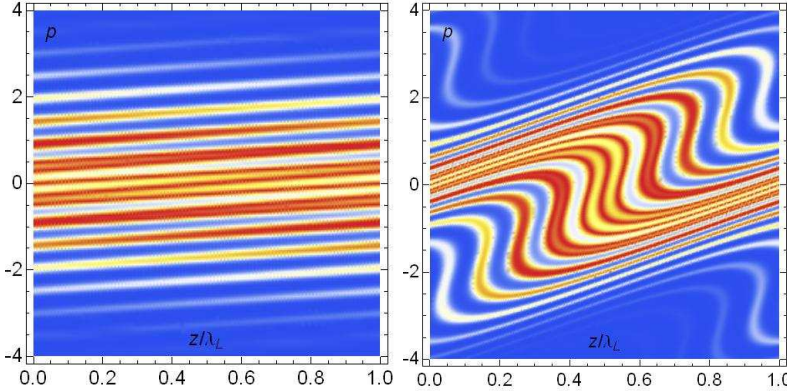


Figure 3. Longitudinal phase space of the beam after passage through the first chicane (left panel) and after passing through the second chicane (right panel). The vertical axis shows the dimensionless deviation of the energy $p = (E - E_0)/\sigma_E$, and the horizontal axis is the longitudinal coordinate z normalized by the laser wavelength λ_L .

4. PRACTICAL CONSIDERATIONS

There are some practical considerations that were neglected in the simple one-dimensional model of EEHG developed in the previous sections. Among the most important are the incoherent synchrotron radiation (ISR) and the coherent synchrotron radiation (CSR) of the beam in dipole magnets of the dispersive elements of the system.

Due to the relatively large dispersion strength in the first chicane ISR may affect the performance of the echo seeding. The mechanism responsible for suppression of EEHG is diffusion in energy due to quantum fluctuations in the process of radiation. If the rms energy spread caused by this diffusion exceeds the spacing of two adjacent energy bands (see left panel of Fig. 3), the bands would overlap and smear out the fine structures of the longitudinal phase space thus degrading the EEHG modulation.

One can easily estimate the energy diffusion by calculating the energy spread $\Delta\sigma_E$ due to passage of a charged particle through a bend of length L and bending radius ρ :⁹

$$\Delta\sigma_E^2|_{ISR} = \frac{55e^2\hbar c}{24\sqrt{3}} \frac{L}{\rho^3} \gamma^7, \quad (6)$$

where γ is the relativistic factor and \hbar is the reduced Planck constant. A quick estimate shows that for the beam energy close to 1 GeV, the bending radius of a few meters and the magnet length of order of a meter, the energy spread due to ISR can be of the order of few kiloelectronvolts, or even as small as a fraction of keV, and typically is smaller than the energy spread of the bands generated in the first chicane. However, a steep dependence of $\Delta\sigma_E$ on the beam energy would limit application of the echo seeding for beam energies of many gigaelectronvolts, unless a weak magnetic field is used in the chicanes (leading to a large length of the seeding system).

If the density modulation of the beam occurs inside the magnets of the chicane, it would cause the coherent synchrotron radiation and a concomitant energy modulation inside the dispersive section, which may result both in the emittance growth of the beam and the distortion of the phase space structures required for the echo modulation. Fortunately, there is a strong suppression effect due to a smearing of such modulation caused by nonzero values of the parameters R_{51} and R_{52} inside the chicanes. Typically, the dominant smearing is due to R_{51} , and the suppression factor for a Gaussian transverse beam profile is^{10,11} $e^{-k_{mod}^2 R_{51}^2 \sigma_x^2 / 2}$, where k_{mod} is the wave number of the modulation and σ_x is the transverse rms size of the bunch in the magnet. For representative numbers $\sigma_x \sim 40 \mu\text{m}$, $R_{51} \approx 0.01$, one finds that modulation with the wavelengths less than $\sim 1 \mu\text{m}$ will be extinguished and hence the CSR will be suppressed.

One has to keep in mind, however, that for non-Gaussian distribution functions the suppression may not be so effective as for the Gaussian distribution. It is also important to understand that the mechanism behind

the suppression is reversible, and an unwanted beam modulation may recover at a downstream location in the accelerator lattice.¹² Overall, the issue of CSR effects in EEHG might require further theoretical and experimental studies.

There are also other requirements on the system that should be satisfied in order not to destroy a small-scale echo microbunching. They are discussed in more detail in Refs.^{8,13,14} Some issues of the noise amplification in the process of EEHG seeding was addressed in.¹⁵

5. PERFORMANCE OF THE EEHG FEL

To illustrate a possible performance of the EEHG FEL we will use an example of Ref.¹⁶ where a feasibility of coherent soft x-ray generation in the water window with the EEHG scheme was studied for the beam parameters based on the high repetition rate soft x-ray FEL under design at LBNL.¹⁷ The parameters of the model are summarized in Table 1. The study assumed the seed laser wavelength of 190 nm with the EEHG FEL operating

Table 1. Main beam parameters

Electron beam energy	2.411 GeV
Peak current	1 kA
Normalized emittance	0.7 mm mrad
Slice energy spread	95 keV
Modulator period length	20 cm
Seed laser peak power	110 MW
Radiator period length	4 cm

at the 50th harmonic of the laser. In order to limit the dispersion strength of the chicanes to a moderate value to mitigate the incoherent synchrotron radiation effect while not degrading the FEL performance, the dimensionless modulation amplitudes were chosen: $A_1 = 3$ and $A_2 = 6$.

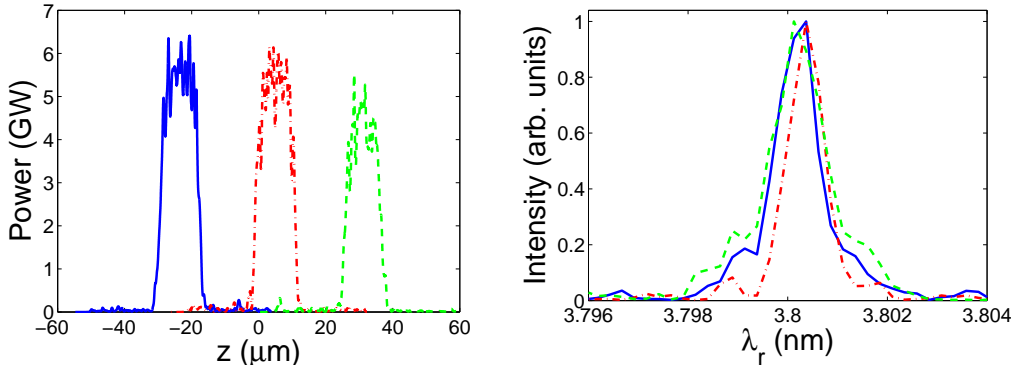


Figure 4. (a) Power profiles corresponding to different seed positions along the bunch; (b) Corresponding spectrum profiles.

Using the particle distribution obtained in a start-to-end simulation, it was demonstrated that the single-stage EEHG FEL can generate high power soft x-ray radiation in the water window with narrow bandwidth close to the Fourier transform limit directly from a UV seed laser. The output power profiles and spectrums corresponding to 3 different seed positions along the bunch obtained through time-dependent simulation using GENESIS code are shown in Fig. 4. The output pulse length is about 12 fs (rms) and the relative spectral bandwidth is 2.7×10^{-4} , about 1.3 times larger than the Fourier transform limit.

Ref.¹⁸ describes a feasibility study of EEHG seeding of the upgrade of the LCLS x-ray FEL at SLAC. The EEHG option has been also studied for several existing and future FEL facilities: for the FERMI soft x-ray FEL,^{19,20} for the PSI SwissFEL project,²¹ and, more recently, for FLASH-II at DESY.²²

6. PROOF-OF-PRINCIPLE EXPERIMENT AT SLAC

A proof-of-principle experiment to demonstrate EEHG has been recently carried out at SLAC National Accelerator Laboratory. The existing NLCTA facility which houses an S-band photocathode electron gun and an X-band accelerator were used for the experiment. The parameters of the experiment are summarized in Table 2.

Table 2. Main beam and laser parameters

Electron beam energy	120 MeV
Normalized emittance	$\sim 8 \mu\text{m}$
Slice energy spread	$\sim 1 \text{keV}$
First laser wavelength	795 nm
Second laser wavelength	1590 nm

the experiment, the beam was first energy modulated in the first modulator using a Ti:Sapphire laser with the wavelength 795 nm and then sent through a chicane with a strong dispersion. A second laser from the optical parametric amplifier (1590 nm) was used to further modulate the beam energy in the second modulator. The density-modulated beam produced coherent radiation at the diagnostic undulator at the end of the system, which was analyzed with a spectrometer.

Due to the small energy spread of the beam, both the HGHG and EEHG mechanisms of harmonic generation were expected to be observed in the experiment. In order to distinguish between them an energy chirp was introduced in the beam by accelerating it off-crest in RF structures. An example of observed spectrogram and

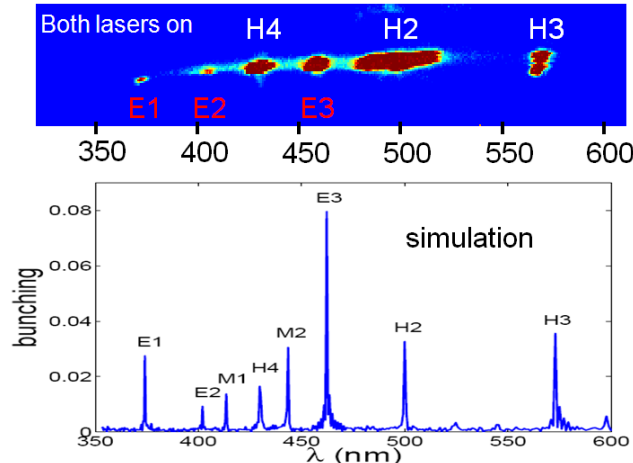


Figure 5. Comparison of the observed spectrogram (the top part of the figure) with simulations (the bottom part). H2, H3, H4 are the HGHG signals, E1, E2, E3 are the EEHG signals identified in simulations, M1, M2 are the EEHG lines seen in simulations, but not in the experiment.

comparison with a simulated spectrum is shown in Fig. 5. The lines are shifted from their nominal positions given by Eq. (1) due to the energy chirp. One can see that all observed in the experiment lines were properly identified in the simulation. Two extra lines in simulations (M1 and M2) were missing in the experiment, which is explained by the fact that the lines are sensitive functions of modulation amplitudes, which were not well known in the experiment.

7. FURTHER DEVELOPMENTS OF THE EEHG CONCEPT AND ITS MODIFICATIONS

In a subsequent development of the EEHG concept, in papers,^{23,24} it was proposed to generate ultrashort pulses of x-ray radiation by adding a few more elements to the original scheme of the echo modulation. In this scheme,

a short undulator is added before the second chicane, with a few-cycle laser beam tuned to the wavelength of the new undulator. The beam interacts in the third undulator with a few-cycle intense laser whose wavelength is chosen to be much longer than that of the laser in the first two undulators, so that part of the electrons around the zero crossing of the few-cycle laser gets almost linear energy chirp. For the parameters considered in,²³ the wavelength of the main seed laser was assumed 200 nm, and the wavelength of the additional laser was 800 nm. The energy of the 800 nm laser was 1 mJ and the pulse length 5 fs. With this additional energy chirp, the beam is longitudinally compressed after passing through the second dispersion section and the harmonic number is increased by the compression factor. In addition to assisting in extension of the harmonic number to a few hundred, the few-cycle laser also offers a possibility to select an isolated attosecond pulse.

In a recent paper²⁵ an echo-based scheme to generate two attosecond x-ray pulses with different carrier frequencies and variable delay has been proposed for x-ray stimulated Raman spectroscopy. Somewhat different approach to generation of attosecond pulses using a modified EEHG mechanism was also considered in.²⁶

Feasibility analysis of a future hard x-ray FEL based on a two-stage EEHG concept can be found in Ref.²⁷ The effective harmonic number in this approach is equal to 1200, leading to the final seeding at 0.15 nm from the initial laser wavelength of 180 nm. A similar cascaded EEGH scheme is used in²⁸ to generate 600th harmonic of the laser wavelength.

A modification of the echo scheme²⁹ can be used to generate enhanced narrow-band terahertz (THz) radiation through down-conversion of the frequency of optical lasers using laser-modulated electron beams. In this scheme the frequencies of the lasers ω_1 and ω_2 are chosen in such a way that for some integers n and m the combination frequency $\omega = n\omega_1 + m\omega_2$ correspond to the terahertz frequency range. This means that one can generate density modulation at THz frequency in the beam using optical lasers. Such a density-modulated beam can then be used to generate powerful narrow-band THz radiation. Since the THz radiation is in tight synchronization with the lasers, it should provide a high temporal resolution for the optical-pump THz-probe experiments. The central frequency of the THz radiation can be easily tuned by varying the wavelength of the two lasers and the energy chirp of the electron beam. The proposed scheme is in principle able to generate intense narrow-band THz radiation covering the whole THz range and offers a promising way towards the tunable intense narrow-band THz sources.

An idea to replace the external laser power sources in the EEHG modulators with FEL oscillators was proposed in.³⁰ It relies on 50-70% reflective dielectric mirrors in the range of few tens of nanometers with the goal to generate longitudinally coherent FEL radiation at ~ 1 nm. Simulation carried out in³⁰ demonstrated feasibility of such scheme at the level of ~ 300 MW with 80th harmonic of 215 nm of the external laser at the final wavelength 1.12 nm.

There was some interest to employ EEHG in rings. In the paper³¹ the authors studied a modification of the slicing technique which would allow generation of ultra-short pulses of coherent radiation at the SOLEIL light sources. A more challenging approach in³² seeks to create steady-state microbunching in the beam of a storage ring to produce coherent radiation at a high repetition rate or in continuous mode.

Finally, in Ref.³³ the authors considered a modification of EEGH in which the first stage uses the emittance exchange unit instead of the traditional modulator-chicane scheme.

8. CONCLUSIONS

The echo-enhanced harmonic generation provides a promising way to introduce a controlled density modulation in an electron beam at a high harmonic of the laser frequency. It opens new possibilities in generation of coherent soft x-rays from free electron lasers, with an option that includes extremely short, attosecond-duration pulses.

ACKNOWLEDGMENTS

The author would like to thank his collaborator Dao Xiang, who made crucial contributions to many subjects covered in this report.

This work was supported by the U.S. Department of Energy contract DE-AC02-76SF00515.

REFERENCES

1. C. Pellegrini, "X-ray free-electron lasers and ultrafast science at the atomic and molecular scale," in *Proc. European Particle Accelerator Conference, Edinburgh, 2006*, pp. 3636–3639, 2006.
2. A. Kondratenko and E. Saldin, "Generation of coherent radiation by a relativistic electron beam in an undulator," *Particle Accelerators* **10**, pp. 207–216, 1980.
3. R. Bonifacio, C. Pellegrini, and L. M. Narducci, "Collective instabilities and high-gain regime in a free electron laser," *Optics Communications* **50**, pp. 373–378, 1984.
4. R. Bonifacio, L. D. S. Souza, P. Pierini, and E. T. Scharlemann, "Generation of XUV light by resonant frequency tripling in a two-wiggler FEL amplifier," *Nucl. Instrum. Meth. A* **296**, pp. 787–790, 1991.
5. L. Yu, "Generation of intense uv radiation by subharmonically seeded single-pass free-electron lasers," *Phys. Rev. A* **44**, p. 5178, 1991.
6. J. Wu and L. H. Yu, "Coherent hard x-ray production by cascading stages of high gain harmonic generation," *Nuclear Instruments and Methods A* **475**, pp. 104–111, 2001.
7. G. Stupakov, "Using the beam-echo effect for generation of short-wavelength radiation," *Phys. Rev. Lett.* **102**, p. 074801, 2009.
8. D. Xiang and G. Stupakov, "Echo-enabled harmonic generation free electron laser," *Phys. Rev. ST Accel. Beams* **12**, p. 030702, 2009.
9. A. W. Chao and M. Tigner, *Handbook of Accelerator Physics and Engineering*, World Scientific, Singapore, 3d ed., 2006.
10. S. Heifets, G. Stupakov, and S. Krinsky, "Coherent synchrotron radiation instability in a bunch compressor," *Phys. Rev. ST Accel. Beams* **5**, p. 064401, 2002.
11. Z. Huang and K.-J. Kim, "Formulas for coherent synchrotron radiation microbunching in a bunch compressor chicane," *Phys. Rev. ST Accel. Beams* **5**, p. 074401, 2002.
12. Z. Huang *et al.*, "Measurements of the LCLS laser heater and its impact on the LCLS FEL performance," in *Proceedings of the 2009 FEL Conference, paper WEOA01*, (Liverpool, UK), 2009.
13. Z. Huang, D. Ratner, G. Stupakov, and D. Xiang, "Effects of energy chirp on echo-enabled harmonic generation free electron lasers," in *Proceedings of the 2009 FEL Conference*, p. 127, (Liverpool, UK), 2009.
14. D. Xiang and G. Stupakov, "Tolerance study for the echo-enabled harmonic generation free electron laser," in *Proceedings of the 2009 Particle Accelerator Conference*, p. 2367, (Vancouver, Canada), 2009.
15. G. Stupakov, Z. Huang, and D. Ratner, "Noise amplification in echo-enabled harmonic generation (EEHG)," in *Proceedings of the 2010 FEL Conference*, p. 278, (Malmö City, Sweden), 2010.
16. D. Xiang and G. Stupakov, "Coherent soft x-ray generation in the water window with the EEHG scheme," in *Proceedings of the 2009 Particle Accelerator Conference*, p. 2327, (Vancouver, Canada), 2009.
17. J. Corlett *et al.*, "Design Studies for a VUV Soft X-ray Free-Electron Laser Array," *Synchrotron Radiation News* **22**, 2009.
18. D. Xiang and G. Stupakov, "Echo-seeding options for LCLS-II," in *Proceedings of the 2010 FEL Conference*, p. 282, (Malmö City, Sweden), 2010.
19. E. Allaria, X. Dao, and G. D. Ninno, "Feasibility studies for single stage echo-enabled harmonic in FERMI FEL-2," in *Proceedings of the 2010 FEL Conference*, p. 39, (Malmö City, Sweden), 2010.
20. E. Allaria and G. D. Ninno, "Implementation of single-stage echo-enabled harmonic generation on the FERMI@ELETTRA FEL," in *Proceedings of the 2010 FEL Conference*, p. 354, (Malmö City, Sweden), 2010.
21. S. Reiche, R. Abela, H.-H. Braun, B. Patterson, and M. Pedrozzi, "Seeding option for the soft x-ray beamline of SwissFEL," in *Proceedings of the 2009 FEL Conference*, p. 51, (Liverpool, UK), 2009.
22. H. Deng, W. Decking, and B. Faatz, "The echo-enabled harmonic generation options for flash ii," Tech. Rep. <http://arxiv.org/ftp/arxiv/papers/1103/1103.0112.pdf>, DESY, 2011.
23. D. Xiang, Z. Huang, and G. Stupakov, "Generation of intense attosecond x-ray pulses using ultraviolet laser induced microbunching in electron beams," *Phys. Rev. ST Accel. Beams* **12**, p. 060701, 2009.
24. D. Xiang, Z. Huang, and G. Stupakov, "Generation of attosecond x-ray pulses beyond the atomic unit using laser induced microbunching in electron beams," in *Proceedings of the 2009 FEL Conference*, p. 196, (Liverpool, UK), 2009.

25. A. Zholents and G. Penn, "Obtaining two attosecond pulses for X-ray stimulated Raman spectroscopy," *Nuclear Instruments and Methods in Physics Research A* **612**, pp. 254–259, 2010.
26. J. Yan, H.-X. Deng, D. Wang, and Z.-M. Dai, "EEHG-assisted FEL schemes for attosecond X-ray pulses generation," *Nuclear Instruments and Methods in Physics Research A* **621**, p. 97104, 2010.
27. D. Xiang, Z. Huang, and G. Stupakov, "Feasibility study for a seeded hard x-ray source based on a two-stage echo-enabled harmonic generation FEL," in *Proceedings of the 2009 FEL Conference*, p. 192, (Liverpool, UK), 2009.
28. C. Feng and Z. Zhao, "Coherent hard X-ray free-electron laser based on echo-enabled staged harmonic generation scheme," in *Proceedings of the First International Particle Accelerator Conference*, p. 2120, (Kyoto, Japan), 2010.
29. D. Xiang and G. Stupakov, "Enhanced tunable narrow-band thz emission from laser-modulated electron beams," *Phys. Rev. ST Accel. Beams* **12**, p. 080701, 2009.
30. J. Wurtele, G. Penn, M. Reinsch, P. Gandhi, X. Gu, J. Wurtele, K.-J. Kim, R. Lindberg, and A. Zholents, "Tunable soft X-ray oscillator," in *Proceedings of the 2010 FEL Conference*, p. 315, (Malmö City, Sweden), 2010.
31. C. Evain, M.-E. Couplie, J.-M. Filhol, M. Labat, A. Nadji, and A. Zholents, "Study of high harmonic generation at synchrotron SOLEIL using an echo enabling technique," in *Proceedings of the First International Particle Accelerator Conference*, p. 2308, (Kyoto, Japan), 2010.
32. D. F. Ratner and A. W. Chao, "Steady-state microbunching in a storage ring for generating coherent radiation," *Phys. Rev. Lett.* **105**, p. 154801, 2010.
33. B. Jiang, J. G. Power, R. Lindberg, W. Liu, and W. Gai, "Emittance-exchange-based high harmonic generation scheme for a short-wavelength free electron laser," *Phys. Rev. Lett.* **106**, p. 114801, 2011.